BUTTERWORTH
HEINEMANN

Polymer Vol. 36 No. 19, pp. 3739–3743, 1995
Copyright © 1995 Elsevier Science Ltd
Printed in Great Britain. All rights reserved
0032-3861/95/$10.00+0.00

Phonon dispersion in poly(α-aminoisobutyric acid)

Onkar Prasad, Poonam Tandon, V. D. Gupta* and Shantanu Rastogi
Physics Department, Lucknow University, Lucknow 226 007, India
(Received 21 October 1994)

The present work is a study of phonons and their dispersion in poly(α-aminoisobutyric acid) (PAIB), which is an example of a poly(amino acid) having a 3_{10} helical conformation. PAIB has been used as a model to carry out conformational studies on proteins and polypeptides. Dispersion curves show two interesting opposite features: (1) a tendency of some curves to crowd or close in near $\delta = \psi$,which is indicative of coupling between various modes, and (2) a divergence of some dispersion curves belonging to species of the same symmetry. The specific heat is obtained from the dispersion curves via the density of states.

(Keywords: conformation; phonon dispersion; density of states)

INTRODUCTION

As a part of the ongoing research work on vibrational analysis and phonon dispersion for numerous biopolymers[1–9], in the present communication we report similar studies on poly(α-aminoisobutyric acid) (PAIB). In addition, the specific heat has been obtained, which has a theoretically predicted value. Dwivedi and Krimm[10] have already reported Raman and infra-red (i.r.) spectroscopic studies and normal mode calculations (without dispersion) for PAIB. A study of phonon dispersion is essential because it facilitates a correlation between the macroscopic properties of a crystal, such as the specific heat, enthalpy, entropy, free energy, etc., and its microscopic behaviour.

PAIB belongs to the class of poly(amino acid)s that exist in the 3_{10} helical conformation. The steric hindrance of the two methyl groups attached to the α-carbon atom forces the dihedral angles to adjust to values very close to those required for right-handed, left-handed 3_{10}, or α helices. Dwivedi and Krimm[10] concluded from their normal mode calculations that PAIB adopts a 3_{10} helical conformation. Recently, Aleman *et al.*[11] have performed molecular mechanical studies of PAIB which also support this conclusion. We have carried out our studies on PAIB assuming the 3_{10} helix to be the most favourable conformation.

THEORY

Calculation of normal mode frequencies

The Higgs-modified GF matrix method of Wilson for an infinite chain has been used as a mathematical tool for calculating the normal mode frequencies [12]. In brief, the vibrational secular equation as a function of the phase angle δ has the form

$$G(\delta)F(\delta) - \lambda(\delta)I = 0, \quad 0 \le \delta \le \pi \tag{1}$$

where G is the inverse kinetic energy matrix, F is the force field matrix and δ is the vibrational phase difference between two successive residue units.

The vibrational frequencies $\nu(\delta)$ in reciprocal centimetres are related to the eigenvalues $\lambda(\delta)$ by

$$\lambda(\delta) = 4\pi^2 c^2 \nu^2(\delta) \tag{2}$$

Calculation of the specific heat

For one-dimensional systems the density of states function which expresses the energy distribution among the various branches of normal modes in the crystal is calculated from

$$g(\nu) = \sum_j (\partial\nu_j/\partial\delta)^{-1}\,|_{\nu_j(\delta)=\nu} \tag{3}$$

Postulating a crystal as an assembly of harmonic oscillators, the frequency distribution becomes equivalent to the partition function. The constant volume specific heat capacity can be calculated using Debye's equation

$$C_{\mathrm{v}} = \sum_j g(\nu_j) k N_{\mathrm{A}} (h\nu_j/kT)^2 \frac{\exp(h\nu_j/kT)}{[\exp(h\nu_j/kT) - 1]^2} \tag{4}$$

with

$$\int g(\nu_j)\,\mathrm{d}\nu_{\mathrm{j}} = 1$$

RESULTS AND DISCUSSION

In PAIB there are 13 atoms per residue, giving rise to 39 dispersion curves. The vibrational frequencies were calculated for different δ values in the interval 0–π in

---

* To whom correspondence should be addressed

Table 1 Internal coordinates and force constants (mdyn Å^{-1})^{a}

ν(C=N)	6.100	ϕ(O=C–Cα)	0.660 (0.60)
ν(C=O)	7.300	ϕ(O=C=N)	0.450 (0.90)
ν(Cα–C)	3.350	ϕ(Cα–C=N)	0.750 (0.60)
ν(Cα–N)	3.628	ϕ(Cα–Cβ_1–Hβ_1)	0.440 (0.35)
ν(H–N)	5.260	ϕ(Cα–C β_2–Hβ_2)	0.440 (0.35)
ν(Cβ_1–Hβ_1)	4.310	ϕ(Hβ_1–Cβ_1–Hβ_1)	0.375 (0.26)
ν(Cβ_2–Hβ_2)	4.310	ϕ(Hβ_2–Cβ_2–Hβ_2)	0.375 (0.26)
ν(Cβ_1–Cα)	3.400	ϕ(Cβ_1–Cα–Cβ_2)	0.600 (0.24)
ν(Cβ_2–Cα)	3.400		
ϕ(H–N=C)	0.315 (0.60)	ω(N–H)	0.080
ϕ(C=N–Cα)	0.725 (0.35)	ω(C=O)	0.640
ϕ(H–N–Cα)	0.230 (0.51)		
ϕ(N–Cα–Cβ_1)	0.300 (0.45)	τ(Cα–C)	0.020
ϕ(N–Cα–Cβ_2)	0.300 (0.45)	τ(C=N)	0.100
ϕ(N–Cα–C)	0.980 (1.50)	τ(Cα–Cβ_1)	0.0095
ϕ(C–Cα–Cβ_1)	0.420 (0.15)	τ(Cα–Cβ_2)	0.0095
ϕ(C–Cα–Cβ_2)	0.420 (0.15)	τ(N–Cα)	0.006

[a] Note that ν, ϕ, ω and τ denote stretch, angle bend, wag and torsion, respectively. Non-bonded force constants are given in parentheses

steps of 0.05π. The modes corresponding to $\delta = 0, \psi$ and 2ψ are optically active, where ψ is the angle of rotation about the helix axis which separates the adjacent units. For PAIB the value of ψ is $2\pi/3$. All the modes above 1350 cm^{-1} except amide I and II are non-dispersive, and hence only modes below this are shown later in *Figures 2a* and *3a*. The force constants which give the best fit to the experimental data of Dwivedi and Krimm[10] are given in *Table 1*. The assignments of normal mode frequencies were made on the basis of potential energy distributions (PEDs) and previous assignments given by Dwivedi and Krimm[10]. The calculated and observed frequencies (at $\delta = 0$ and $2\pi/3$) along with their assignments are given in *Table 2*. The two lowest-lying branches ($\delta = 0$ and $\delta = 2\pi/3$, $\nu = 0$) are four acoustic modes which correspond to the rotation about the helix axis and translations parallel and perpendicular to the helix axis. For the sake of simplicity the modes are discussed in two separate sections, *viz.* backbone and side-chain modes.

Side-chain modes

The side chain of PAIB consists of two methyl groups attached to the α-carbon atom (Cα) (*Figure 1*). Our calculated methyl stretches, both symmetric and asymmetric, match closely the observed frequencies (*Table 2*).

The calculated asymmetric CH_3 bendings at 1441, 1437, 1435 and 1433 cm^{-1} are assigned to the two observed frequencies at 1457 and 1450 cm^{-1}, the resolution of which into four peaks is limited by the experimental techniques employed. The CH_3 symmetric bendings are observed at 1386 and 1364 cm^{-1} and the calculated ones are assigned within 15–22 cm^{-1} as given in *Table 2*. All CH_3 rocking modes except the one at 954 cm^{-1} (calculated) match closely the observed frequencies. This mode assigned to the observed frequency at 923 cm^{-1} could not be better fitted in spite of our best efforts which involved taking into account the off-diagonal coupling constants.

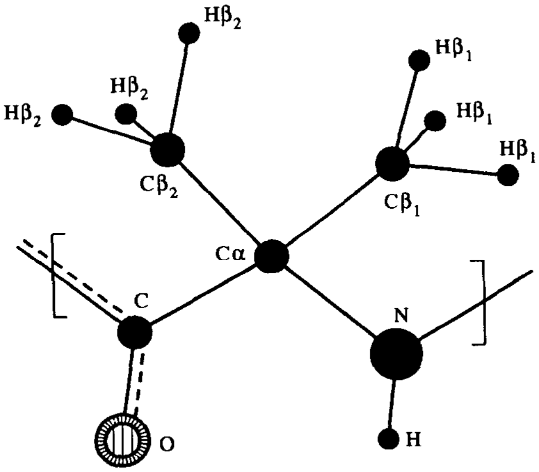

Figure 1 Repeat unit of poly(α-aminoisobutyric acid)

Backbone modes

Modes involving the motion of main-chain atoms (–C–Cα–N–) are termed backbone modes. These modes are marked with an asterisk in *Table 2*. Amide groups of polypeptides are strong chromophores in i.r. absorption and these groups give rise to strong characteristic bands (amide A and I–VII). The correlations between these characteristic bands and conformations have been found to be useful for conformational diagnosis of polypeptides.

The amide A band arising from N–H stretching is characteristic of its functional group. This mode is highly sensitive to the strength of N–H···O=C hydrogen bonding. Our calculated amide A frequency at 3264 cm^{-1} is assigned to the observed one at 3260 cm^{-1}, which is somewhat lower than the N–H stretch in the α-helix form (around 3290 cm^{-1}), reflecting stronger hydrogen bonding and weaker N–H bonding. This is further supported by the fact that the N···O distance in the case of the 3_{10} helix is 2.83 Å, but in the case of α-helical polypeptides this distance is 2.93–3 Å.

All the amide modes except amide A are found to be dispersive. Amide IV shows maximal dispersion (60 cm^{-1}). It has 48% contribution from C=O in-plane bending. With increasing δ, the energy of this mode and the contribution of C=O in-plane bending decrease, whereas ω(N–H) starts to make an increasing contribution to the PED. As seen from the dispersion curves (see later) the modes at frequencies of 578 and 570 cm^{-1} at $\delta = 0$ diverge from each other in such a fashion that these modes interchange PED contributions, i.e. C=O in-plane bending increases but ϕ(N–Cα–C) decreases in the former mode, whereas these coordinates have the reverse trend in the case of the latter mode. The energy of

Table 2 Calculated and observed modes of poly(α-aminoisobutyric acid) (asterisk indicates backbone mode)

Calculated (cm^{-1})	Observed (cm^{-1})	Assignment (% PED at $\delta = 0$)		Calculated (cm^{-1})	Observed (cm^{-1})	Assignment (% PED at $\delta = 2\pi/3$)	
3264	3260*	ν(N–H)(99)	(Amide A)	3264	3260	ν(N–H)(99)	(Amide A)
2984	2985	ν(Cβ_1–Hβ_1)(52) + ν(Cβ_2–Hβ_2)(47)		2984	2995	ν(Cβ_1–Hβ_1)(52) + ν(Cβ_2–Hβ_2)(47)	
2984		ν(Cβ_1–Hβ_1)(47) + ν(Cβ_2–Hβ_2)(52)		2984		ν(Cβ_1–Hβ_1)(47) + ν(Cβ_2–Hβ_2)(52)	
2933	2933	ν(Cβ_1–Hβ_1)(49) + ν(Cβ_2–Hβ_2)(49)		2933	2935	ν(Cβ_1–Hβ_1)(49) + ν(Cβ_2–Hβ_2)(49)	
2932		ν(Cβ_1–Hβ_1)(47) + ν(Cβ_2–Hβ_2)(52)		2932		ν(Cβ_1–Hβ_1)(47) + ν(Cβ_2–Hβ_2)(51)	
2932		ν(Cβ_1–Hβ_1)(52) + ν(Cβ_2–Hβ_2)(47)		2932		ν(Cβ_1–Hβ_1)(51) + ν(Cβ_2–Hβ_2)(47)	
2931		ν(Cβ_1–Hβ_1)(49) + ν(Cβ_2–Hβ_2)(49)		2932		ν(Cβ_1–Hβ_1)(49) + ν(Cβ_2–Hβ_2)(49)	
1670	1656*	ν(C=O)(45) + ν(C=N)(30) + ϕ(N–Cα–C)(6) + ϕ(Cα–C=N)(6)	(Amide I)	1651	1656	ν(C=O)(49) + ν(C=N)(29) + ϕ(Cα–C=N)(6)	(Amide I)
1534	1531*	ν(N–Cα)(8) + ν(Cα–C)(15) + ν(C=N)(21) + ϕ(C=N–H)(20) + ϕ(H–N–Cα)(15)	(Amide II)	1505	1545	ν(N–Cα)(12) + ν(Cα–C)(12) + ν(C=N)(22) + ϕ(C=N–H)(20) + ϕ(H–N–Cα)(14)	(Amide II)
1441	1457	ϕ(Hβ_1–Cβ_1–Cα)(6) + ϕ(Hβ_1–Cβ_1–Hβ_1)(41) + ϕ(Hβ_2–Cβ_2–Cα)(6) + ϕ(Hβ_2–Cβ_2–Hβ_2)(42)		1444	1455	ϕ(Hβ_1–Cβ_1–Cα)(6) + ϕ(Hβ_1–Cβ_1–Hβ_1)(36) + ϕ(Hβ_2–Cβ_2–Cα)(7) + ϕ(Hβ_2–Cβ_2–Hβ_2)(39)	
1437		ϕ(Hβ_1–Cβ_1–Cα)(8) + ϕ(Hβ_1–Cβ_1–Hβ_1)(72) + ϕ(Hβ_2–Cβ_2–Hβ_2(13)		1439		ϕ(Hβ_1–Cβ_1–Cα)(7) + ϕ(Hβ_1–Cβ_1–Hβ_1)(53) + ϕ(Hβ_2–Cβ_2–Hβ_2)(27)	
1435	1450	ϕ(Hβ_1–Cβ_1–Hβ_1)(13) + ϕ(Hβ_2–Cβ_2–Cα)(8) + ϕ(Hβ_2–Cβ_2–Hβ_2)(74)		1435	1450	ϕ(Hβ_1–Cβ_1–Hβ_1)(30) + ϕ(Hβ_2–Cβ_2–Cα)(6) + ϕ(Hβ_2–Cβ_2–Hβ_2)(58)	
1433		ϕ(Hβ_1–Cβ_1–Hβ_1)(46) + ϕ(Hβ_2–Cβ_2–Hβ_2)(45)		1433		ϕ(Hβ_1–Cβ_1–Hβ_1)(47) + ϕ(Hβ_2–Cβ_2–Hβ_2)(43)	
1393	1386	ϕ(Hβ_1–Cβ_1–Cα)(7) + ϕ(Hβ_1–Cβ_1–Hβ_1)(6) + ϕ(Hβ_2–Cβ_2–Cα)(47) + ϕ(Hβ_2–Cβ_2–Hβ_2)(35)		1396	1385	ϕ(Hβ_1–Cβ_1–Cα)(20) + ϕ(Hβ_1–Cβ_1–Hβ_1)(18) + ϕ(Hβ_2–Cβ_2–Cα)(27) + ϕ(Hβ_2–Cβ_2–Hβ_2)(22)	
1389	1364	ϕ(Hβ_1–Cβ_1–Cα)(47) + ϕ(Hβ_1–Cβ_1–Hβ_1)(35) + ϕ(Hβ_2–Cβ_2–Cα)(6) + ϕ(Hβ_2–Cβ_2–Hβ_2)(5)		1392	1364	ϕ(Hβ_1–Cβ_1–Cα)(30) + ϕ(Hβ_1–Cβ_1–Hβ_1)(23) + ϕ(Hβ_2–Cβ_2–Cα)(24) + ϕ(Hβ_2–Cβ_2–Hβ_2)(19)	
1318	1313	ν(Cα–C)(12) + ν(C=O)(7) + ϕ(C=N–H)(14) + ϕ(H–N–Cα)(17) + ν(Cα–Cβ_2)(20)	(Amide III)	1351	–	ν(Cα–Cβ_1)(8) + ν(Cα–C)(25) + ϕ(C=N–H)(7) + ϕ(H–N–Cα)(10) + ϕ(Hβ_1–Cβ_1–Cα)(6) + ϕ(Hβ_1–Cβ_1–Hβ_1)(6) + ν(Cα–Cβ_2)(5) + ϕ(Hβ_2–Cβ_2–Hβ_2)(5)	
1262	1280	ν(N–Cα)(38) + ν(Cα–C)(22) + ϕ(Hβ_1–Cβ_1–Cα)(9) + ϕ(Hβ_2–Cβ_2–Cα)(8)		1311	1304	ν(N–Cα)(32) + ϕ(H–N–Cα)(5) + ϕ(Hβ_1–Cβ_1–Cα)(5) + ϕ(Hβ_1–Cβ_1–Hβ_1)(5) + ν(Cα–Cβ_2)(16) + ϕ(Hβ_2–Cβ_2–Cα)(5) + ϕ(Hβ_2–Cβ_2–Hβ_2)(5)	
1236	1230	ν(Cα–Cβ_1)(49) + ϕ(Hβ_2–Cβ_2–Cα)(12)		1228	1227	ν(Cα–Cβ_1)(39) + ν(Cα–Cβ_2)(19) + ϕ(Hβ_2–Cβ_2–Cα)(8)	
1192	1210	ν(C=O)(5) + ν(C=N)(15) + ϕ(C=N–H)(6) + ϕ(H–N–Cα)(6) + ϕ(Hβ_1–Cβ_1–Cα)(13) + ν(Cα–Cβ_2)(33)		1161	1170	ν(N–Cα)(5) + ν(C=O)(12) + ν(C=N)(16) + ϕ(Hβ_1–Cβ_1–Cα)(16) + ν(Cα–Cβ_2)(8) + ϕ(Hβ_2–Cβ_2–Cα)(11)	
1004	1018	ϕ(Hβ_1–Cβ_1–Cα)(42) + ϕ(Hβ_2–Cβ_2–Cα)(47)		1005	1018	ϕ(Hβ_1–Cβ_1–Cα)(42) + ϕ(Hβ_2–Cβ_2–Cα)(48)	
981	996	ν(Cα–Cβ_1)(6) + ϕ(Hβ_1–Cβ_1–Cα)(36) + ν(Cα–Cβ_2)(6) + ϕ(Hβ_2–Cβ_2–Cα)(39)		986	996	ν(N–Cα)(9) + ϕ(Hβ_1–Cβ_1–Cα)(66) + ϕ(Hβ_1–Cβ_1–Hβ_1)(5) + ϕ(Hβ_2–Cβ_2–Cα)(7)	
965	953	ν(N–Cα)(26) + ϕ(Hβ_1–Cβ_1–Cα)(28) + ϕ(Hβ_2–Cβ_2–Cα)(21)		979	–	ν(Cα–Cβ_1)(10) + ϕ(Hβ_2–Cβ_2–Cα)(69) + ϕ(Hβ_2–Cβ_2–Hβ_2)(5)	
954	923	ν(Cα–Cβ_1)(12) + ϕ(Hβ_1–Cβ_1–Cα)(30) + ν(Cα–Cβ_2)(13) + ϕ(Hβ_2–Cβ_2–Cα)(28)		955	940	ν(N–Cα)(10) + ν(Cα–C)(5) + ϕ(C=N–Cα)(5) + ϕ(Hβ_1–Cβ_1–Cα)(29) + ν(Cα–Cβ_2)(9) + (Hβ_2–Cβ_2–Cα)(14)	
917	908	ν(Cα–C)(21) + ϕ(C=N–Cα)(8) + ϕ(O=C=N)(9) + ϕ(Hβ_1–Cβ_1–Cα)(5) + ν(C=O)(22) + ϕ(Hβ_2–Cβ_2–Cα)(7)		864	–	ν(N–Cα)(6) + ν(Cα–Cβ_1)(9) + ν(Cα–C)(16) + ν(C=O)(11) + ϕ(O=C=N)(5) + ω(C=O)(9) + ν(Cα–Cβ_2)(16)	
759	762	ν(Cα–Cβ_1)(8) + ω(N–H)(7) + ω(C=O)(73)	(Amide VI)	790	790	ν(Cα–Cβ_1)(18) + ϕ(N–Cα–C)(7) + ω(N–H)(7) + ω(C=O)(48) + ν(Cα–Cβ_2)(6)	(Amide VI)
687	680*	ω(N–H)(31) + τ(N–Cα)(10) + τ(C=N)(46)	(Amide V)	677	694	ω(N–H)(28) + ω(C=O)(7) + τ(N–Cα)(9) + τ(C=N)(49)	(Amide V)
578	595	ν(N–Cα)(8) + ν(Cα–Cβ_1)(12) + ϕ(N–Cα–C)(28) + ν(Cα–C)(6) ϕ(Cβ_1–Cα–Cβ_2)(6) + τ(C=N)(6) + ν(Cα–Cβ_2)(13)		641	642	ν(Cα–C)(13) + ϕ(C=N–Cα)(7) + ϕ(Cα–C=O)(14) + ϕ(O=C=N)(14) + ω(C=O)(7)	(Amide IV)
570	568	ϕ(N–Cα–Cβ_1)(10) + ϕ(Cα–C=O)(40) + ϕ(Cα–C=N)(12) + ϕ(O=C=N)(8) + ϕ(Cβ_1–Cα–C)(7)	(Amide IV)	502	505	ϕN–Cα–C)(31) + ϕ(Cβ_1–Cα–C)(5) + ϕ(Cβ_1–Cα–Cβ_2)(5) + ϕ(Cα–C=N)(5) + ϕ(O=C=N)(7) + ω(C=O)(5) + ν(Cα–Cβ_2)(6) + ϕ(N–Cα–Cβ_2)(11)	
372	362	ϕ(C=N–Cα)(7) + ϕ(N–Cα–C)(7) + ϕ(Cβ_1–Cα–Cβ_2)(15) + ϕ(N–Cα–Cβ_2)(47)		389	367	ϕ(C=N–Cα)(6) + ϕ(Cβ_1–Cα–Cβ_2)(20) + ϕ(Cα–C=O)(14) + ϕ(O=C=N)(5) + ϕ(N–Cα–Cβ_2)(23)	

Table 2 (Continued)

Calculated (cm^{-1})	Observed (cm^{-1})	Assignment (% PED at $\delta = 0$)	Calculated (cm^{-1})	Observed (cm^{-1})	Assignment (% PED at $\delta = 2\pi/3$)
296	298	ϕ(C=N–Cα)(7) + ϕ(N–Cα–Cβ_1)(19) + ϕ(Cβ_1–Cα–C)(7) + ϕ(Cβ_1–Cα–Cβ_2)(10) + ϕ(Cβ_1–Cα–C)(7) + ϕ(Cα–C=O)(6) + ϕ(O=C=N)(18)	305	313	ϕ(N–Cα–Cβ_1)(41) + ϕ(Cβ_1–Cα–Cβ_2)(25) + ϕ(Cα–C=N)(6) + ϕ(O=C=N)(7)
257	–	ν(Cα–C)(6) + ϕ(Cβ_1–Cα–C)(17) + ϕ(Cβ_1–Cα–Cβ_2)(29) + ϕ(O=C=N)(5) + ϕ(N–Cα–Cβ_2)(7) + ϕ(Cβ_1–Cα–C)(18)	273	284	ν(N–Cα)(5) + ϕ(N–Cα–Cβ_1)(6) + ϕ(N–Cα–C)(7) + ϕ(Cβ_1–Cα–C)(11) + ϕ(Cβ_1–Cα–Cβ_2)(21) + ϕ(Cα–C=O)(10) + ϕ(Cα–C=N)(9) + ϕ(N–Cα–Cβ_2)(7)
239	–	ϕ(N–Cα–Cβ_1)(19) + ϕ(Cβ_1–Cα–C)(23) + τ(Cα–Cβ_2)(11) + ϕ(Cα–C=N)(6) + ϕ(Cβ_1–Cα–C)(5) + ϕ(Cβ_1–Cα–Cβ_2)(13)	226	220	τ(Cα–Cβ_1)(30) + ϕ(N–Cα–Cβ_2)(8) + ϕ(Cβ_1–Cα–C)(34)
220	220	τ(Cα–Cβ_1)(75) + τ(Cα–Cβ_2)(20)	220		τ(Cα–Cβ_1)(28) + τ(Cα–Cβ_2)(65)
215		ϕ(Cβ_1–Cα–C)(8) + τ(Cα–Cβ_1)(15) + τ(Cα–Cβ_2)(67)	213		τ(Cα–Cβ_1)(38) + τ(Cα–Cβ_2)(25) + ϕ(Cβ_1–Cα–C)(18)
162	165	ϕ(C=N–Cα)(7) + ϕ(N–Cα–Cβ_1)(8) + ϕ(N–Cα–C)(8) + ϕ(Cβ_1–Cα–C)(6) + ϕ(Cα–C=N)(5) + τ(Cα–C)(18) + ϕ(N–Cα–Cβ_2)(13) + ϕ(Cβ_1–Cα–C)(12)	177	189	ϕ(N–Cα–Cβ_1)(8) + ϕ(Cβ_1–Cα–C)(37) + ϕ(Cα–C=N)(9) + τ(Cα–C)(7) + ϕ(Cβ_1–Cα–C)(5)
117	115	ϕ(C=N–Cα)(21) + ϕ(N–Cα–Cβ_1)(11) + ϕ(Cα–C=N)(17) + ϕ(O=C=N)(7) + ϕ(Cβ_1–Cα–C)(19)	110	107	ϕ(C=N–Cα)(24) + ϕ(N–Cα–C)(6) + ϕ(Cα–C=N)(5) + ω(N–H)(9) + τ(Cα–C)(11) + ϕ(N–Cα–Cβ_2)(13)
82	107*	ϕ(C=N–Cα)(8) + τ(N=Cα)(24) + τ(Cα–C)(49) (Amide VII)	74	–	ϕ(C=N–Cα)(5) + ω(N–H)(9) + τ(N–Cα)(13) + τ(Cα–C)(43) + τ(C=N)(10) (Amide VII)

the higher mode increases and that of the lower mode decreases with increasing δ.

The amide V band, which is predominantly ω(N–H), has been calculated at 687 cm^{-1}, corresponding to the observed peak at 680 cm^{-1}. In the α-helix it is observed around 620 cm^{-1}. Thus the hydrogen bond between N–H and C=O (N–H···C=O) is stronger in PAIB, supporting a more compact helix (3_{10} as opposed to 18_5). Stronger hydrogen bonding leads to an increased N–H out-of-plane bending frequency because of the increased force constant.

The amide VII band, which arises from torsional motion about C=N, also plays an important role in the characterization of conformations. This mode is calculated at 82 cm^{-1}, corresponding to the observed peak at 107 cm^{-1}. At $\delta = 0$ this mode largely consists of τ(Cα–C) and τ(N–Cα); the PED at $\delta = \psi$ shows considerable mixing with τ(C=N). In addition, because of the helical nature of the conformation a certain amount of mixing with ϕ(C=N–Cα) takes place. Such mixing has been reported in the case of the α-form of poly(L-alanine) (α-PLA) but not in the case of the β-form of poly(L-alanine) (β-PLA)[2,3]. Dispersion for this mode is found to be very similar to that for α-PLA. Unlike this mode in β-PLA, there is a decrease in mode frequency with increasing δ from 0 to π.

Amide III, IV and VI do not appear as pure backbone modes. The PEDs of these modes have considerable contributions from the side chain. The frequencies of these amide modes do not depend solely on the main-chain conformation, the side-chain structure in question also playing an important role[13].

Dispersion curves

Dispersion curves (*Figures 2a and 3a*) provide information on the extent and degree of coupling. Two interesting features are observed in the dispersion curves: (1) a tendency of some curves to crowd or close in near $\delta = \psi$, which is indicative of coupling between various modes, and (2) a divergence of some dispersion curves in the neighbourhood of the phase angle, which is a multiple of half the helical angle. The phenomenon of crowding has been observed for two pairs of modes. The first pair consists of the mode at 578 cm^{-1} and amide V. At $\delta = 0$ the former has small contributions from C=O in-plane and out-of-plane bendings which later increase with δ. In the case of amide V the C=O in-plane bending increases at the cost of ω(N–H). The second pair consists of the mode at 117 cm^{-1} (at $\delta = 0$) and amide VII. In the case of the mode at 117 cm^{-1} the contribution of ϕ(C=N–Cα) increases appreciably up to $\delta = 0.6\pi$ and decreases on further increase in δ, whereas for amide VII the PED contribution of the ϕ(C=N–Cα) term decreases with increasing δ. This feature is possibly due to N–H and C=O interaction. All these modes involve the motion of the nitrogen atom. This characteristic feature has been noticed for polytetrafluoroethylene (15/7)[14] and α-PLA (18/5)[2], and has been attributed in both cases to strong intramolecular interactions stabilizing the helical structure.

The second interesting feature of the dispersion curves is the divergence of some modes. The modes at 257 and 296 cm^{-1} for $\delta = 0$ come close together around $\delta = 0.55\pi$ and then diverge. Both these modes are a mixture of bending around Cα and C=O in-plane bending. They

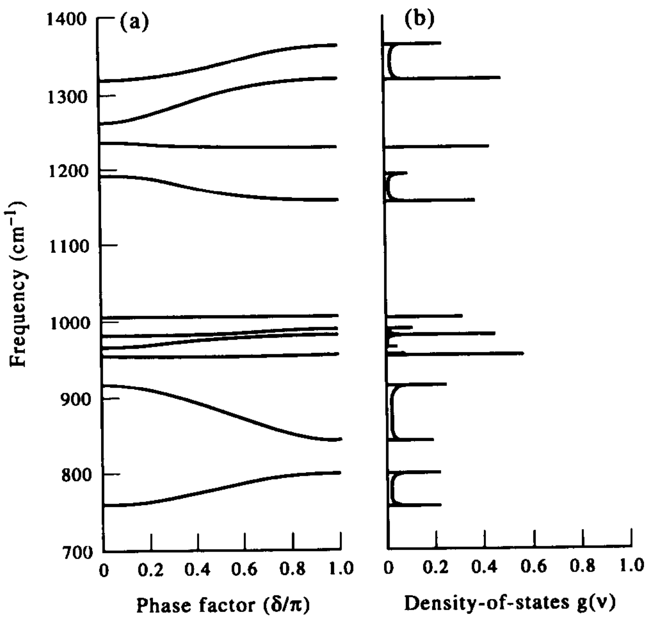

Figure 2 (a) Dispersion curves of poly(α-aminoisobutyric acid) (1400–700 cm^{-1}). (b) Density of states $g(\nu)$ (1400–700 cm^{-1})

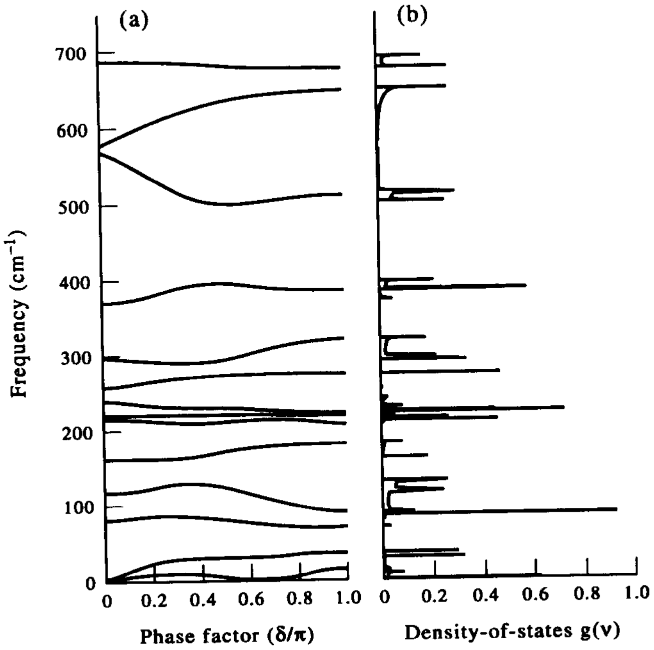

Figure 3 (a) Dispersion curves of poly(α-aminoisobutyric acid) below 750 cm^{-1}. (b) Density of states $g(\nu)$ below 750 cm^{-1}

have the same symmetry. For the 296 cm^{-1} mode the contribution of bending around Cα increases and that of C=O in-plane bending decreases with increasing δ whereas the 257 cm^{-1} mode has the reverse trend. This is another example of the divergence of modes having the same symmetry. Such divergence has recently been observed by Burman *et al.*[8] and Gupta *et al.*[9] in ω-helical polypeptides.

Specific heat

Calculated frequency distributions as a function of frequency are shown in *Figures 2b* and *3b*. The specific heat has been calculated as a function of temperature from the dispersion curves via the density of states. The theoretical details have already been given. The predicted values of the specific heat are shown in *Figure 4*, curve D. The contributions of pure backbone (*Figure 4*, curve A), pure side chain (*Figure 4*, curve B) and mixed modes (*Figure 4*, curve C) to the specific heat have also been calculated. Our results show that the maximum contribution comes from the mixed modes.

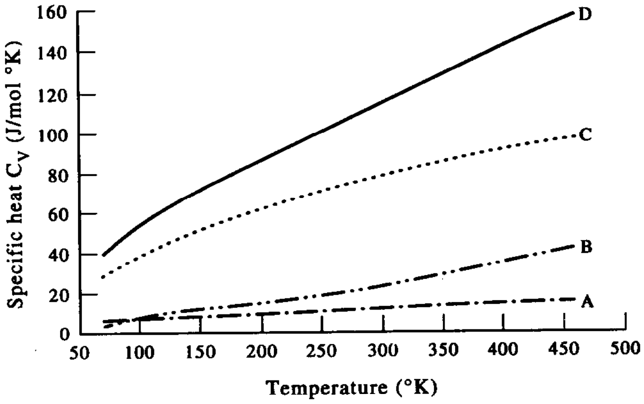

Figure 4 Variation in specific heat C_v with temperature

In spite of several limitations involved in the calculation of the specific heat and the absence of experimental data, the present work provides a good starting point for further basic studies on the thermodynamic behaviour of polypeptide proteins which have well-defined conformations.

ACKNOWLEDGEMENT

Financial assistance to one of the authors (V.D.G.) from CSIR under the Emeritus Scientist Scheme is gratefully acknowledged.

REFERENCES

1 Gupta, V. D., Trevino, S. and Boutin, H. *J. Chem. Phys.* 1968, **48**, 3008
2 Krishnan, M. V. and Gupta, V. D. *Chem. Phys. Lett.* 1970, **6**, 231
3 Krishnan, M. V. and Gupta, V. D. *Chem. Phys. Lett.* 1970, **7**, 285
4 Singh, R. D. and Gupta, V. D. *Spectrochim. Acta, Part A* 1971, **27**, 385
5 Dwivedi, A. M. and Gupta, V.D. *Chem. Phys. Lett.* 1972, **16**, 909
6 Gupta, V. D., Singh, R. D. and Dwivedi, A. M. *Biopolymers* 1973, **12**, 1377
7 Srivastava, R. B and Gupta, V. D. *Biopolymers* 1974, **13**, 1965
8 Burman, L., Tandon, P., Gupta, V. D., Rastogi, S., Srivastava, S. and Gupta, G. P. *J. Phys. Soc. Jpn* 1995, **64**, 307
9 Gupta, A., Tandon P., Gupta, V. D., Rastogi, S. and Gupta, G. P. *J. Phys. Soc. Jpn* 1995, **64**, 315
10 Dwivedi, A. M. and Krimm, S. *Biopolymers* 1984, **23**, 2025
11 Aleman, C., Subirana, J. A. and Perez, J. J. *Biopolymers* 1992, **32**, 621
12 Higgs, P. W. *Proc. R. Soc. London, Ser. A* 1953, **220**, 472
13 Krimm, S. and Bandekar, J. *Adv. Protein Chem.* 1986, **38**, 181
14 Hannon, M. J., Boerio, F. J. and Koenig, J. L. *J. Chem. Phys.* 1969, **50**, 2829